biomimetics

MDPI

Article

Design and Analysis of a Polymeric Left Ventricular Simulator via Computational Modelling

Turgut Batuhan Baturalp [1,*] and Selim Bozkurt [2,*]

[1] Department of Mechanical Engineering, Texas Tech University, P.O. Box 41021, Lubbock, TX 79409, USA
[2] School of Engineering, Ulster University, York Street, Belfast BT15 1AP, UK
* Correspondence: b.baturalp@ttu.edu (T.B.B.); s.bozkurt1@ulster.ac.uk (S.B.)

Abstract: Preclinical testing of medical devices is an essential step in the product life cycle, whereas testing of cardiovascular implants requires specialised testbeds or numerical simulations using computer software Ansys 2016. Existing test setups used to evaluate physiological scenarios and test cardiac implants such as mock circulatory systems or isolated beating heart platforms are driven by sophisticated hardware which comes at a high cost or raises ethical concerns. On the other hand, computational methods used to simulate blood flow in the cardiovascular system may be simplified or computationally expensive. Therefore, there is a need for low-cost, relatively simple and efficient test beds that can provide realistic conditions to simulate physiological scenarios and evaluate cardiovascular devices. In this study, the concept design of a novel left ventricular simulator made of latex rubber and actuated by pneumatic artificial muscles is presented. The designed left ventricular simulator is geometrically similar to a native left ventricle, whereas the basal diameter and long axis length are within an anatomical range. Finite element simulations evaluating left ventricular twisting and shortening predicted that the designed left ventricular simulator rotates approximately 17 degrees at the apex and the long axis shortens around 11 mm. Experimental results showed that the twist angle is 18 degrees and the left ventricular simulator shortens 5 mm. Twist angles and long axis shortening as in a native left ventricle show it is capable of functioning like a native left ventricle and simulating a variety of scenarios, and therefore has the potential to be used as a test platform.

Keywords: left ventricle; left ventricular simulator; pneumatic artificial muscle

Citation: Baturalp, T.B.; Bozkurt, S. Design and Analysis of a Polymeric Left Ventricular Simulator via Computational Modelling. *Biomimetics* **2024**, *9*, 269. https://doi.org/10.3390/biomimetics9050269

Academic Editors: Andrew Adamatzky, Benliang Zhu and Hai Li

Received: 17 March 2024
Revised: 12 April 2024
Accepted: 27 April 2024
Published: 28 April 2024

1. Introduction

Preclinical testing of medical devices is an essential step in the product life cycle [1], whereas testing of cardiovascular implants such as valve substitutes or continuous flow left ventricular assist devices requires specialised testbeds or numerical simulations using computer software [2,3]. For instance, a transcatheter aortic valve was tested considering ISO standards to evaluate clinical performance using a patient-specific in vitro test setup [4]. The hydrodynamic performance of a transcatheter mitral valve was evaluated using a commercial pulse duplicator [5]. Surgical and transcatheter pulmonary valve devices have also been tested using in vitro setups [6,7]. Specialised test setups have also been used to simulate clinical scenarios and left ventricular assist device support. For instance, Rocchi et al. studied suction incidents caused by a left ventricular assist device to validate clinical data using a test bench [8]. A novel continuous flow left ventricular assist device flow rate control algorithm to improve arterial pulsatility was tested using a mock circulatory system [9]. Test setups simulating cardiac function in these studies are actuated using pistons driven by complex systems and drivers; therefore, these setups are costly [10].

Ex vivo passive beating experimental cardiac models provide anatomical geometries in the testing of cardiovascular devices [11–13]. Heart valve function during left ventricular assist device support was evaluated using a passive beating experimental cardiac model [14]. Heart valve biomechanics can also be tested in these setups [15]. Moreover,

measurements, such as chordae tendineae tension, which cannot be collected easily in vivo in the mitral valve apparatus can be collected using additional sensors in the ex vivo systems [16]. Nonetheless, passive beating heart platforms or ex vivo heart valve models also require actuators, which consist of pistons and complex drivers to generate the cardiac signals over an entire cardiac cycle. Therefore, although passive beating heart platforms provide advantages, such as working with anatomical structure, their actuation system has similar limitations to mock circulatory systems.

Isolated beating heart platforms do not need external actuators because the electrical activity of the heart is preserved during the experiments [17,18]. Isolated beating heart platforms can be used to evaluate a variety of scenarios, such as continuous flow left ventricular assist device support [19,20], heart valve performance [21], and myocardial perfusion [22] or they can be used as a training tool [23]. Nonetheless, experimental data show that a lack of autoregulatory mechanisms in isolated hearts may result in relatively high heart rates and continuous hyperemia [24,25].

Animal models provide realistic conditions for the clinical cases [26–28]. Therefore, animal models have been used to evaluate cardiovascular devices. For instance, sheep or bovine models were used to evaluate a centrifugal flow left ventricular assist device [29–31]. Animal models have also been used to develop and test prosthetic heart valve devices [32]. However, increasing ethical concerns and developments in computational models established roadmaps to refine, reduce, and replace animal experiments [33–35].

Lumped and distributed parameter models have been used in cardiovascular research to evaluate clinical cases and cardiovascular devices [36]. Lumped parameter models simulate blood flow rates and pressures in different compartments of the cardiovascular system; therefore, they are suitable for simulating the whole cardiovascular system over a relatively short period [37–39]. For instance, the evaluation of cardiac function and blood flow in the cardiovascular system during left ventricular assist device support and atrial fibrillation is presented in [40]. Nonetheless, lumped parameter models provide information only about pressures and blood flow rates in the cardiovascular system. Computational fluid dynamics models are used to simulate blood flow velocities and related parameters such as wall shear stresses in the cardiovascular system [41]. Computational fluid dynamics models have been used in heart valve and continuous flow left ventricular assist device research [42,43]. Although computational fluid dynamics simulations provide detailed information about the blood flow in an anatomical structure, they may be computationally expensive [44–46].

It is clear that there is a need for low-cost, relatively simple and efficient test beds that can provide realistic conditions to simulate physiological scenarios and evaluate cardiovascular devices. The aim of this study is to design and analyse a left ventricle simulator resembling native left ventricular geometry and simulating left ventricular wall motion in a realistic way.

2. Materials and Methods

The shape and dimensions of the left ventricle chamber were selected considering anatomical ranges of basal diameter and long axis length in a healthy heart. The left ventricular basal diameter changes between 39 mm and 56 mm and the long axis length changes between 90 mm and 104 mm [47–49]. Therefore, the left ventricular basal diameter was 45 mm, whereas the long axis length was 97 mm in the geometric model. The diameter of the left ventricle model was reduced along the long axis to 40 mm and the apex of the left ventricle model was created using a radius curve tangent to the horizontal axis. The volume of the left ventricle model was 118 mL within the physiological end-diastolic left ventricle volume over a cardiac cycle [50,51]. A line geometry revolved around the vertical axis to create a 1 mm thick left ventricle chamber. The thickness of the left ventricle model was decided considering the mechanical properties of latex rubber [52]. The section curve used to generate the left ventricle wall and the generated left ventricle geometry are given in Figure 1.

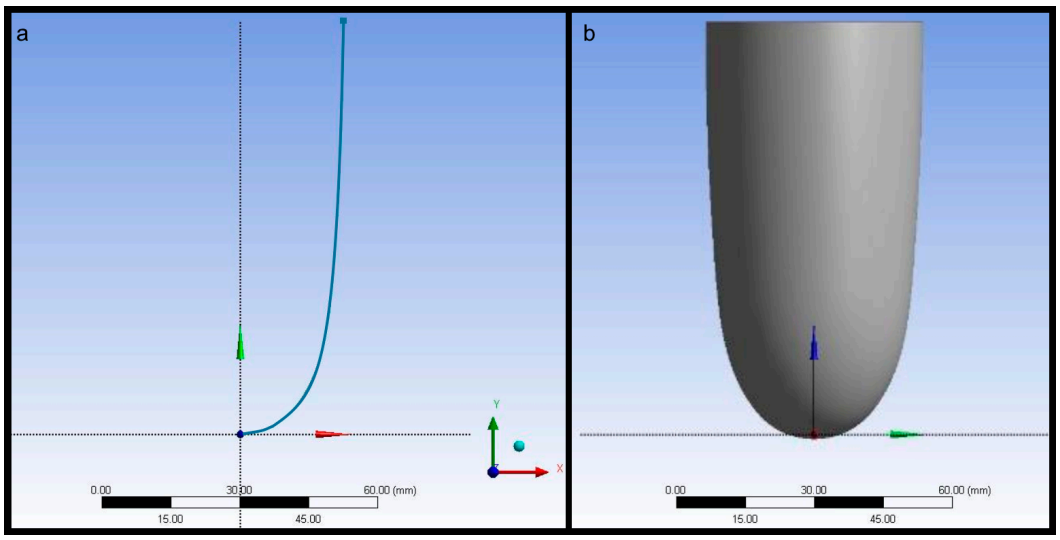

Figure 1. (**a**) The section curve used to generate the left ventricle wall and (**b**) the generated left ventricle geometry.

Pneumatic artificial muscles have been proposed to activate ventricular contraction in cardiac simulators [53]. In this study, a similar activation method was utilised using helical tubes around the left ventricle chamber [54]. The pneumatic artificial muscles in the actual beating left ventricle simulator were positioned in helical orientation to increase the pumping performance with the help of torsional contraction and to mimic the swirling pattern of the cardiac muscles. The general assembly pattern has a 90-degree shift between two ends of the muscles to make installing pneumatic artificial muscles easier. Since projection on two-dimensional space is already a quarter circle, it creates a helical curve when it is projected to a three-dimensional space. However, a helical curve should have conical features to follow the conic geometry of the geometric model. Therefore, a conical spiral was chosen to generate a spiral arrangement of muscles. The general form of parametric equations is given as follows for a conical spiral.

$$x = t \times r \times \cos(a \times t) \tag{1}$$

$$y = t \times r \times \sin(a \times t) \tag{2}$$

$$z = t \tag{3}$$

Here, a is the angular frequency, z is the height of the cone, and r is the radius. The angular range was chosen as 0 to $\pi/2$ radians for a 90-degree shift. MATLAB 2016b (Mathworks, Natick, MA, USA) was used to generate a curve for the conical spiral and as an input file in ANSYS 2016 Design Modeler (ANSYS, Canonsburg, PA, USA). A three-dimensional line body is generated in ANSYS Design Modeler using the generated curve in MATLAB 2016b (Mathworks, Natick, MA, USA). The conical curve was projected onto the geometric models as described above using the projected paths as a guideline for actuator generation. Four pneumatic artificial muscles were generated around the left ventricle chamber so as not to make the left ventricle chamber too stiff during the ejection phase [54]. The input conical spiral in Ansys Design Modeler, a projected curve, and the guidelines to create pneumatic artificial muscle geometries are given in Figure 2.

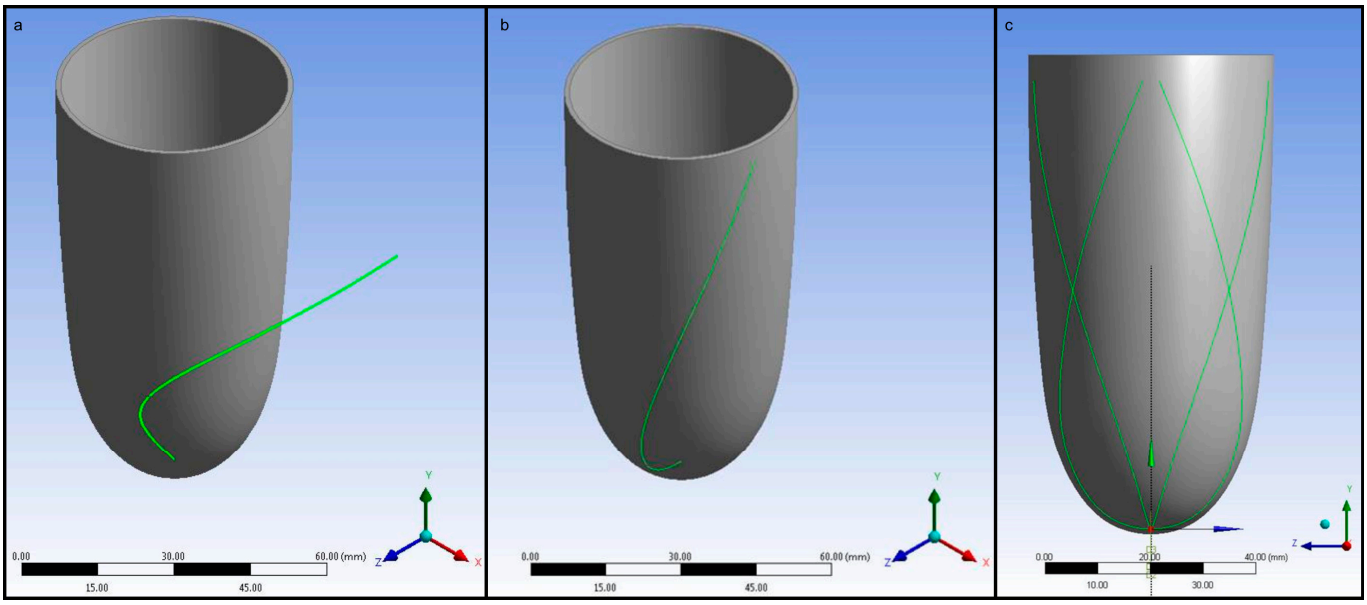

Figure 2. (**a**) The input conical spiral in Ansys Design Modeler, (**b**) a projected curve, and (**c**) the guidelines to create pneumatic artificial muscle geometries.

The pneumatic artificial muscle geometries were generated using the guideline curves utilising Sweep operation in ANSYS Design Modeler. The diameter of the pneumatic artificial muscles was 5 mm in the finite element model. The pneumatic artificial muscles from the isometric and top views are given in Figure 3.

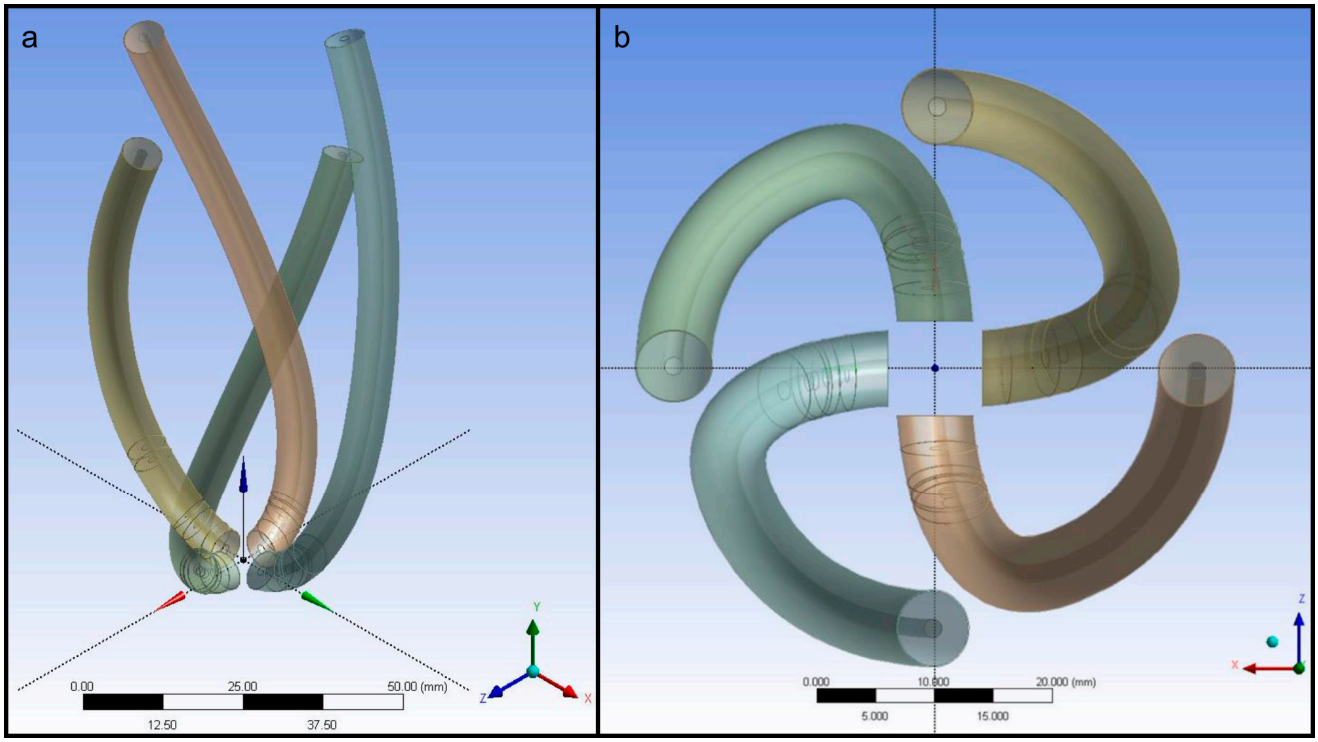

Figure 3. The pneumatic artificial muscles: (**a**) isometric view, (**b**) top view.

The generated pneumatic artificial muscle geometries were subtracted from the left ventricle geometry to remove the material in the left ventricle walls where the pneumatic artificial muscles are positioned. The geometry of the left ventricle chamber with and without pneumatic artificial muscles is given in Figure 4.

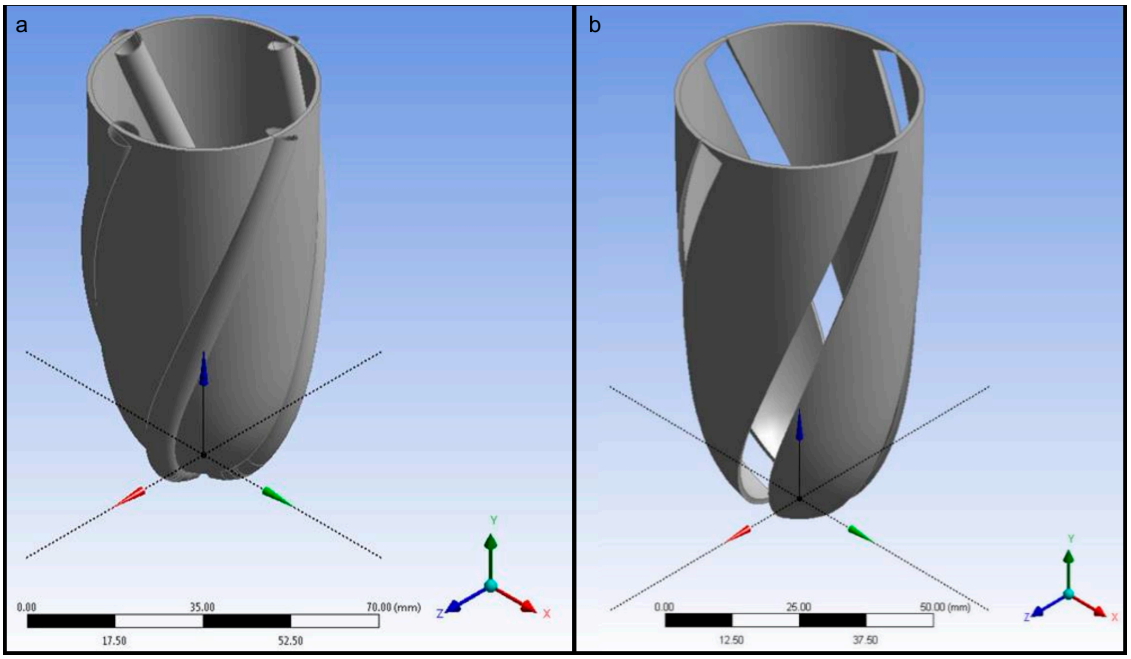

Figure 4. Left ventricle chamber (**a**) with and (**b**) without pneumatic artificial muscles.

The complete model with left ventricle walls and pneumatic artificial muscles was composed of meshed tetrahedral elements. The number of elements in total was around 118,000 after the grid independence test. Pneumatic artificial muscles and ventricle walls were connected using bonded contact. The meshed left ventricular simulator body is given in Figure 5.

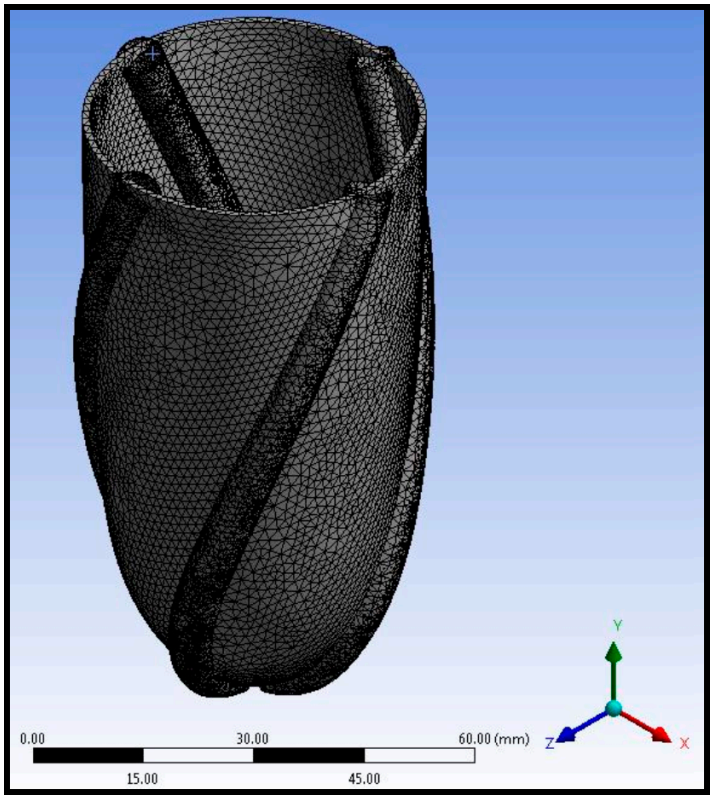

Figure 5. The meshed left ventricular simulator body with ventricle wall and pneumatic artificial muscles.

Linear elastic and isotropic material models for the left ventricle wall and pneumatic actuated muscles were used in the simulations. Latex rubber was considered in the left ventricle wall. Therefore, the Elastic Modulus and Poisson's Ratio of the left ventricle walls were 68.9 kPa and 0.499, whereas the Elastic Modulus of the pneumatic artificial muscles was 1.78 MPa [55] and Poisson's Ratio of the pneumatic artificial muscles was 0.35 [56].

Contraction of the left ventricular simulator was simulated using thermal expansion in the pneumatic artificial muscles. The thermal expansion coefficient of the pneumatic artificial muscles was acquired by an experimental procedure to match the shrinking behaviour of the finite element model of the pneumatic artificial muscle with air pressure expansion, which simulates the cardiac contraction [52]. The equation below was used to determine the thermal expansion coefficient:

$$\Delta L = \alpha \times L \times \Delta T \tag{4}$$

Here, ΔL is the change in the length of a pneumatic artificial muscle, L is the initial length of a pneumatic artificial muscle, ΔT is the change in temperature, and α is the thermal expansion coefficient. The contraction of the ventricle model is driven by the ΔT term and the coefficient α. Because the ΔT term is fixed, it is required to find the correct values of α to achieve realistic results. An arbitrary ΔT of 1000 degrees Celsius is chosen and the thermal expansion coefficient was determined to be 14.36×10^{-5} 1/°C in the finite element model.

A fixed support boundary condition was applied at the base of the left ventricle and the pneumatic artificial muscles considering that the left ventricular simulator will be installed on an experimental setup at the base. The pneumatic artificial muscles were loaded with a thermal condition as described above. Torsional or twisting movement is very important to generate a real left ventricle-like wall motion. Therefore, the "Remote Points" tab was used at the apex of the left ventricle and the outer surface of the left ventricle wall. Boundary conditions used in the geometry of the left ventricular simulator are given in Figure 6.

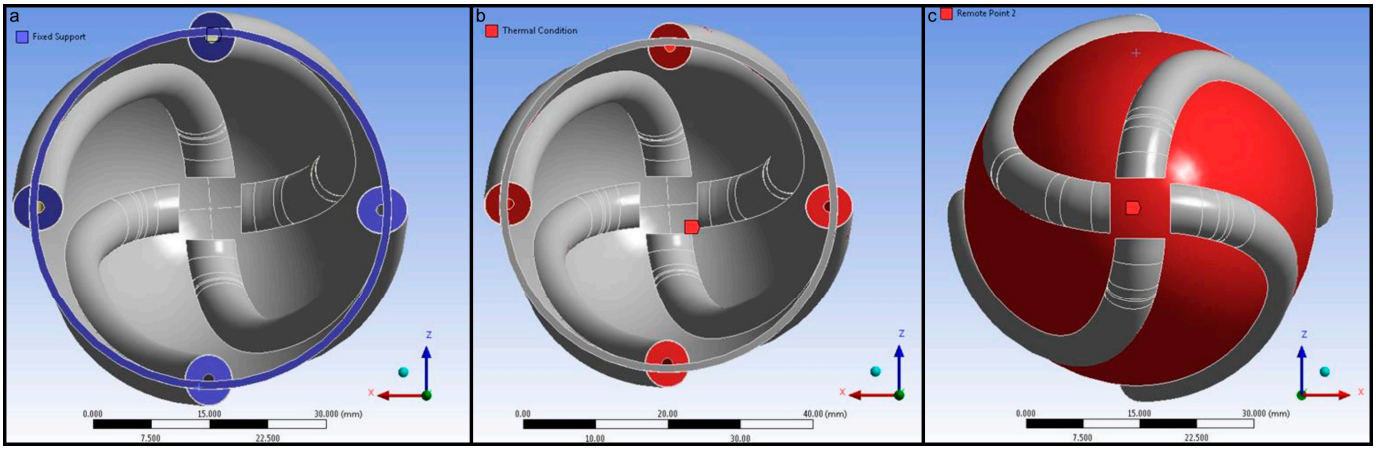

Figure 6. Boundary conditions used in the geometry of the left ventricular simulator: (**a**) fixed support at the upper side of the left ventricle and pneumatic artificial muscles, (**b**) thermal condition in the pneumatic artificial muscles, (**c**) remote point at the apex of the left ventricle and the outer surface of the left ventricle wall.

Prototypes for the left ventricle simulator were built using mould-making latex rubber from AeroMarine Products Inc. (San Diego, CA, USA). Contractions in the left ventricle simulator were actuated using pneumatic artificial muscles, including flexible inner tubes and the braided sleeves. Pneumatic artificial muscles were pressurised using a three-way two-position-type pneumatic electric solenoid to activate the left ventricle chamber over each cycle. The prototyped left ventricle models were fixed on a holder at their base, as simulated in the finite element analyses. The air pressure was set to 80 psi, because higher

air pressures in the pneumatic artificial muscles caused damage to ventricle walls made of latex rubber.

3. Results

The left ventricular contraction was evaluated considering the shortening of the left ventricular long axis and torsion of the pneumatic artificial muscles. The shortening of the left ventricular long axis is given in Figure 7.

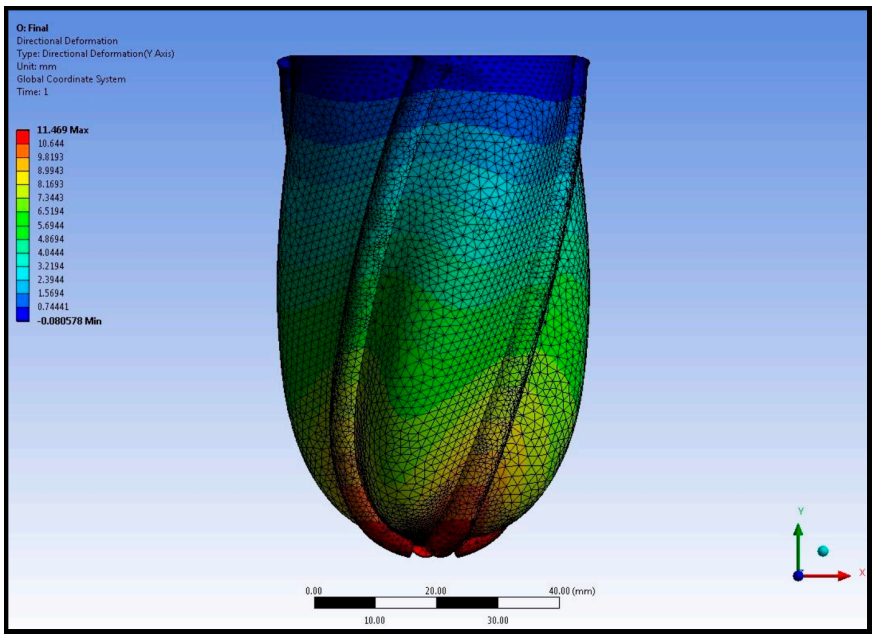

Figure 7. Shortening of the left ventricular long axis in the left ventricular simulator.

Maximal left ventricular shortening was around 11 mm at the apex of the left ventricle. The shortening of the left ventricle around the left ventricular mid-axis was nearly 5 mm. A comparison between the original left ventricular geometry and the deformed left ventricular geometry is given in Figure 8.

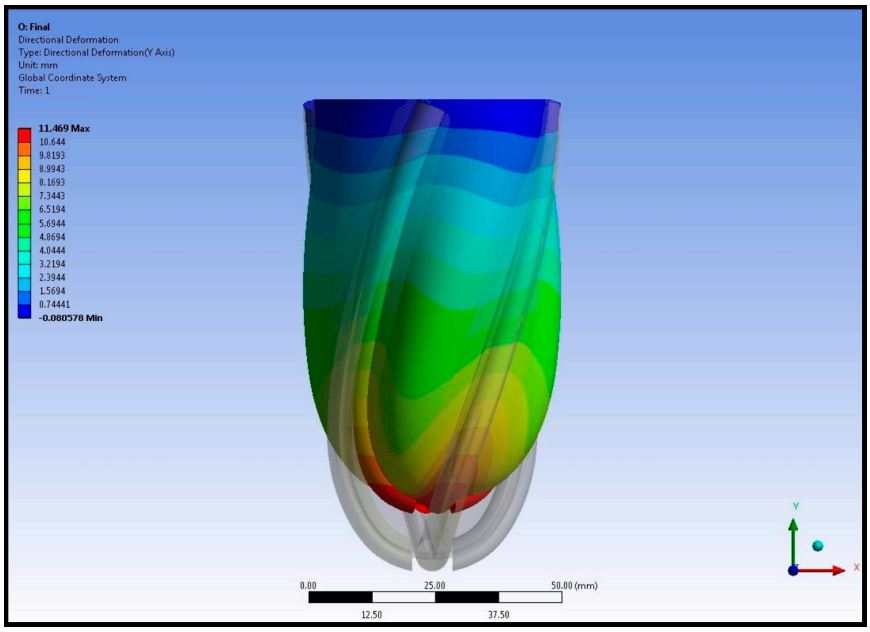

Figure 8. Comparison between the original left ventricular geometry and the deformed left ventricular geometry.

The displacement of the left ventricular wall and pneumatic artificial muscles is shown in Figure 8. Contraction of the pneumatic artificial muscles shortens the left ventricle at the apex. A comparison of original and deformed left ventricle geometries at the left ventricular mid-section from the top view is given in Figure 9.

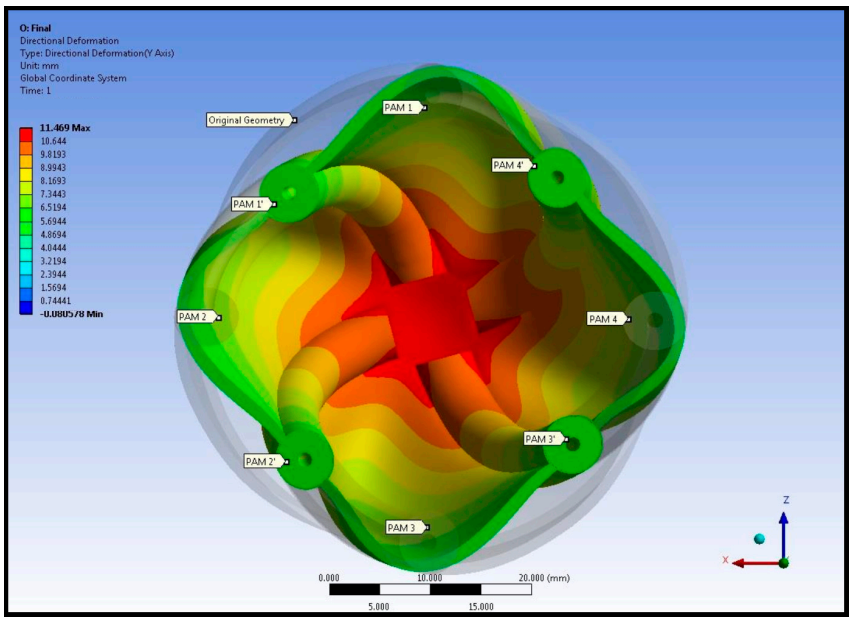

Figure 9. Comparison of original and deformed left ventricle geometries at the left ventricular mid-section from the top view.

Results in Figure 9 show the left ventricular torsion. The orientation of pneumatic artificial muscles was altered by twisting in a counterclockwise direction. Moreover, the shape of the elastomer body is also altered. Because the elastomer body is not thermally loaded, deformation on the body should be a consequence of thermal loading, in other words, contraction of pneumatic artificial muscles. Displacement and rotation in the pneumatic artificial muscles together with a comparison of relaxed pneumatic artificial muscles are given in Figure 10.

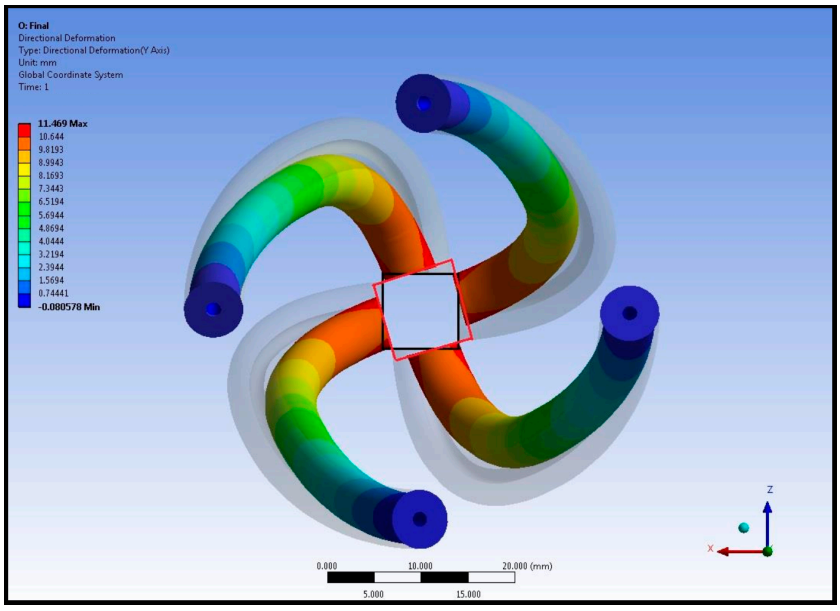

Figure 10. Comparison of the displacement and rotation in the pneumatic artificial muscles in the free and deformed left ventricular model.

The results show how pneumatic artificial muscles undergo deformation, whereas the transparent silhouette shows the original pneumatic artificial muscle shapes. The unloaded pneumatic artificial muscle orientation creates a hypothetical rectangle in the apex region. In addition to the initial rectangle shown in black in Figure 10, the red rectangle depicts the hypothetical rectangle in between the deformed apex. The twist angle of the apex of the left ventricle model was calculated by using the defined triangles. Torsional movement is essential to generate actual human left ventricle-like wall motion and its existence is ensured. Finite element analysis predicted a rotation at the apex of around 17 degrees and an average rotation in the elastomer body at around 7 degrees. A side view of a prototyped left ventricular chamber in free and deformed configurations during a dry run is given in Figure 11.

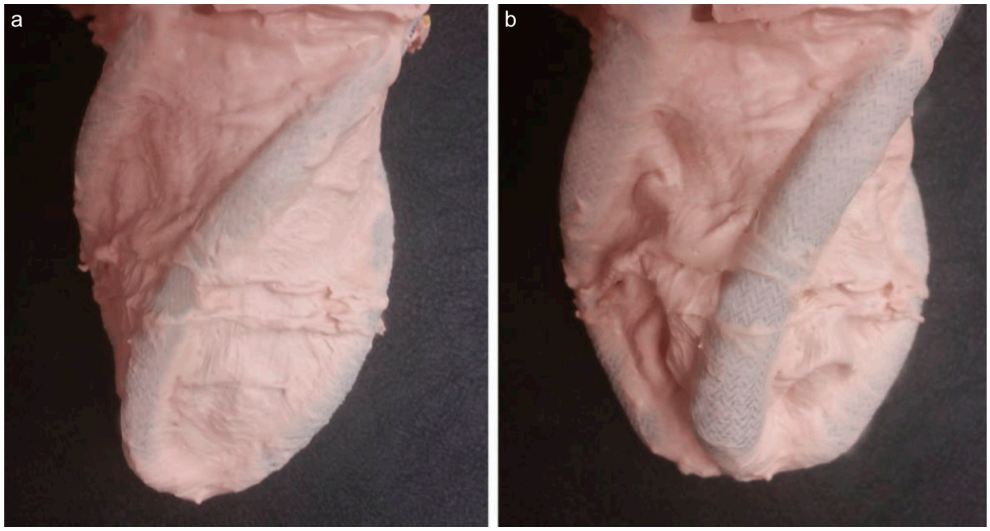

Figure 11. Side view of a prototype of the left ventricular chamber: (**a**) free left ventricular geometry (**b**), deformed left ventricular geometry due to pressurised pneumatic artificial muscles.

Pressurised pneumatic artificial muscles shorten and twist the left ventricular chamber. The shortening of the left ventricle chamber was around 5 mm. The twist angle in a prototype of the left ventricle model during a dry run is given in Figure 12.

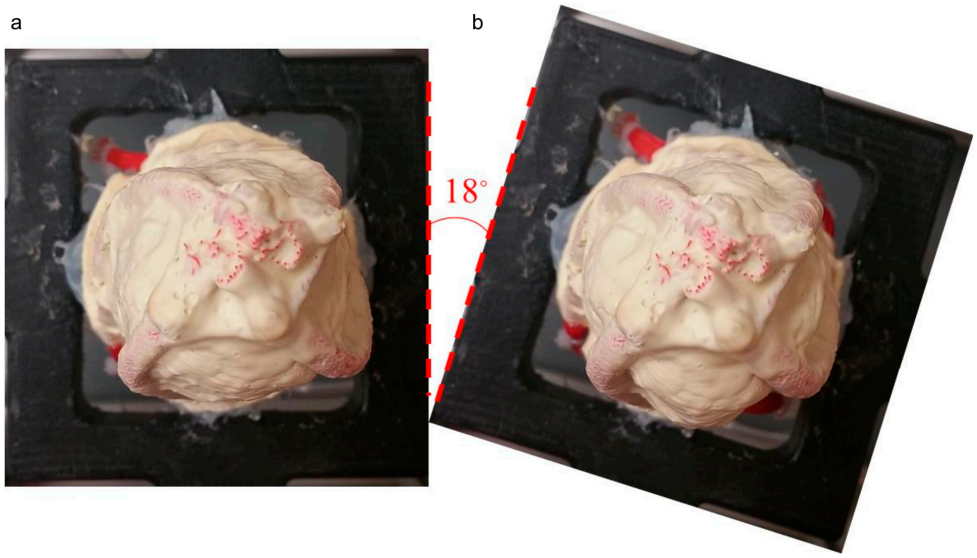

Figure 12. Inferior view of a prototype of the left ventricular chamber: (**a**) free left ventricular geometry, (**b**) deformed left ventricular geometry due to pressurised pneumatic artificial muscles.

The twist angle in the left ventricle model was calculated by rotating the image of the deformed geometry until the orientation of the pneumatic artificial muscles matched with the original undeformed geometry. Twist angle in the left ventricle chamber was around 18 degrees.

4. Discussion

In this study, a novel left ventricular simulator was designed and finite element simulations were performed to evaluate the contractile behaviour of the developed left ventricular simulator. Static structural and thermal simulations were performed to understand the deformation in the left ventricle wall made of latex rubber. Also, prototype production of the proposed left ventricular simulator was carried out to evaluate the validity of the simulations. The developed system is activated by four pneumatic artificial muscles by simply pressurising them using air. A solenoid can control the airflow in the system. Moreover, torsional movement of the left ventricular wall can be replicated because of the orientation of the pneumatic artificial muscles in the system. The proposed left ventricular simulator can be manufactured using simple moulds and commercially available polymeric materials such as latex rubber, as shown in this study. Therefore, the developed system is affordable and easy to manufacture and drive, unlike the sophisticated pulse duplicators, which require high-cost hardware to operate the system [10].

The motion of the left ventricle wall is crucial for the effective pumping function of the left ventricle. Moreover, the torsional movement of the left ventricle is achieved via the helical orientation of myocardial fibres [57–60]. The simulations revealed that the contractile behaviour of the designed left ventricular simulator can imitate the native left ventricular wall deformations in a contracted state. A realistic wall motion in the designed left ventricular simulator was also verified by the twisting angle at the apex. Apical to the basal rotation angle of a healthy ventricle is around 16 degrees [61], whereas maximal long axis shortening in a healthy ventricle is around 10 mm [47]. The simulation results showed that the designed left ventricular simulator rotates around 17 degrees at the apex and shortens 11 mm. Moreover, experimental results show that the twist angle and apex shortening are around 18 degrees and 5 mm. Therefore, the wall motion and torsion in the developed left ventricular simulator are comparable to a healthy ventricle.

Torsional deformation in the native left ventricle is a result of fibre orientation in the ventricle wall [62,63]. Helical flow patterns in the aorta are generated by the torsional deformation of the left ventricular wall and aortic valve angle [64]. The developed left ventricular simulator may generate helical flow patterns at the outlet of the left ventricle because of its design. Flow patterns in aortic valve substitutes may cause complications such as thrombus formation and preclinical testing of these devices requires specialised techniques such as particle image velocimetry [65,66]. However, due to the operating principles of the pulse duplicator, the generated flow patterns in the left ventricle and left ventricular outlet site may not be realistic. Therefore, the developed system in this study may help overcome the challenges of testing the heart valve substitutes before clinical applications.

Previously, cardiac assist devices driven by pneumatic artificial muscles were developed. Roche et al. [67] proposed a soft robotic sleeve driven by pneumatic artificial muscles. Despite the actuator design being somewhat similar to the designed left ventricular simulator, the primary aim of the designed platform in this study is to simulate cardiac function. Lorenzon et al. [68] proposed a left ventricle pump driven by inverse pneumatic artificial muscles. In this design, the inverse pneumatic artificial muscles drove the left ventricle with external helical contraction. In the developed system in this study, the pneumatic artificial muscles were embedded in the left ventricular wall to contract the left ventricle model instead of squeezing it.

The designed ventricular simulator has the following advantages over the existing mock circulatory systems: haemodynamic signals in pulse duplicators generated by piston motion [69,70]. Therefore, physiological effects such as septal shift during mechanical circulatory support may not be simulated in these systems [71–74]. For instance, a developed

mock circulatory system includes both ventricles in a series connection driven by piston pumps [75]. Therefore, it can only simulate haemodynamic signals during left ventricular assist device support. However, the designed left ventricular simulator is capable of simulating left ventricular wall motion because it is made of a flexible material. This may be particularly useful for developing next-generation left ventricular assist devices or testing different configurations during mechanical circulatory support in clinical cases such as cardiogenic shock [76,77]. Beating heart platforms may provide realistic test conditions to evaluate physiological cases [78,79]. However, the use of animal models and animal tissue in research raises ethical concerns [80–83]. The designed left ventricular simulator may help reduce the use of animal models in experiments because the geometry of the left ventricle can be made anatomical and it can replicate left ventricular wall motion.

Dilated and hypertrophic cardiomyopathies are major causes of functional and anatomical remodelling in the left ventricle [84–86]. Dilated cardiomyopathy causes the left ventricle to enlarge, whereas the left ventricular muscle is thinned [87–90]. Hypertrophic cardiomyopathy may cause the left ventricular muscle to thicken [91–93]. Prototyping the left ventricular chambers in different sizes and thicknesses will allow for the simulation of dilated and hypertrophic cardiomyopathies, whereas traditional mock circulatory systems can only simulate left ventricular function. Moreover, left ventricular torsion may increase in the elderly and heart failure results in abnormal left ventricular mechanics [94–96]. All these effects can be simulated by modifying pneumatic artificial muscles in the developed left ventricular simulator. Other potential applications in this system also include testing of heart valve replacement implants where an anatomical shape will result in more accurate tests [97,98]. Patient-specific left ventricular models can also be manufactured and may provide benefits for cohorts such as paediatric patients. Diagnostic criteria in paediatric patients for heart failure are adapted from adults because of the limited available information for children [99,100]. The designed left ventricular simulator can simulate paediatric ventricles and may help to study clinical conditions in this cohort. Moreover, it may be possible to develop personalised models, which allow us to work on personalised patient-specific solutions for patients. However, it should be noted that this study presents the design approach and the concept of the left ventricular simulator.

The developed and tested left ventricular simulator made of flexible latex rubber also has potential for educational and training purposes in the field of cardiovascular medicine and biomedical engineering. The proposed setup may offer a tangible representation of cardiac anatomy and physiology unlike numerical models, which may be inaccessible or challenging to interpret for students and clinicians without a strong background in mathematics and computational science [101]. Moreover, students can gain practical insights into cardiac mechanics, haemodynamics, and pathology, resulting in a deeper understanding of cardiovascular concepts with experimentation with a physical device which can simulate myocardial motion. Current educational test platforms include passive beating heart platforms for testing, training, and teaching transcatheter therapies [13] or 3D-printed models [102]. The proposed model has the advantages of reducing the use of animal tissue and being flexible compared to the 3D-printed rigid models.

This study has a number of limitations. Hydrodynamic tests were not performed, and only left ventricular wall motion during contraction was analysed. Therefore, the hydrodynamic performance of the developed system remains to be studied. A more complete system including the right ventricle will allow for the study of the interaction between the ventricles. The septal shift is a concern for both ventricles during the continuous flow of left ventricular assist device support and may cause right ventricular failure, as mentioned above. Therefore, a more complete cardiac simulator including left and right ventricles will be manufactured in the future. Also, physiological and clinical scenarios such as cardiomyopathies will be considered in the future. Here, it should be noted that the aim of the study is to analyse and understand the design parameters using finite element simulations and show a proof of concept, manufacturing the prototypes of the proposed left ventricular simulator.

5. Conclusions

In this study, design concepts and finite element simulations are presented for a novel left ventricular simulator made of latex rubber. The simulation and experimental test results show that the designed left ventricular simulator can simulate left ventricular twists and shortening as in a native left ventricle. It combines the advantages of being affordable and manufacturability, the potential to generate realistic flow patterns, and practical applications to use as test and educational tools. It may also help to reduce the use of animal models, which raise ethical concerns. Therefore, it may replace or help to improve the existing test platforms being used for research and education.

Author Contributions: Conceptualization, T.B.B. and S.B.; methodology, T.B.B.; software, T.B.B.; validation, T.B.B. and S.B.; formal analysis, T.B.B. and S.B.; investigation, T.B.B.; resources, T.B.B.; data curation, T.B.B. and S.B.; writing—original draft preparation, T.B.B. and S.B.; writing—review and editing, S.B. All authors have read and agreed to the published version of the manuscript.

Funding: This research received no external funding.

Institutional Review Board Statement: Not applicable.

Data Availability Statement: No new data were created or analysed in this study.

Acknowledgments: The authors acknowledge Utku Gulbulak from the University of Kentucky, College of Medicine for his support in the simulations.

Conflicts of Interest: The authors declare no conflicts of interest.

References

1. Tarricone, R.; Ciani, O.; Torbica, A.; Brouwer, W.; Chaloutsos, G.; Drummond, M.F.; Martelli, N.; Persson, U.; Leidl, R.; Levin, L.; et al. Lifecycle Evidence Requirements for High-Risk Implantable Medical Devices: A European Perspective. *Expert Rev. Med. Devices* **2020**, *17*, 993–1006. [CrossRef]
2. Zhang, B.L.; Bianco, R.W.; Schoen, F.J. Preclinical Assessment of Cardiac Valve Substitutes: Current Status and Considerations for Engineered Tissue Heart Valves. *Front. Cardiovasc. Med.* **2019**, *6*, 72. [CrossRef]
3. Malinauskas, R.A.; Hariharan, P.; Day, S.W.; Herbertson, L.H.; Buesen, M.; Steinseifer, U.; Aycock, K.I.; Good, B.C.; Deutsch, S.; Manning, K.B.; et al. FDA Benchmark Medical Device Flow Models for CFD Validation. *ASAIO J.* **2017**, *63*, 150. [CrossRef]
4. Kovarovic, B.J.; Rotman, O.M.; Parikh, P.; Slepian, M.J.; Bluestein, D. Patient-Specific in Vitro Testing for Evaluating TAVR Clinical Performance—A Complementary Approach to Current ISO Standard Testing. *Artif. Organs* **2021**, *45*, E41–E52. [CrossRef]
5. Bozkurt, S.; Preston-Maher, G.L.; Torii, R.; Burriesci, G. Design, Analysis and Testing of a Novel Mitral Valve for Transcatheter Implantation. *Ann. Biomed. Eng.* **2017**, *45*, 1852–1864. [CrossRef]
6. Rasmussen, J.; Skov, S.N.; Nielsen, D.B.; Jensen, I.L.; Tjørnild, M.J.; Johansen, P.; Hjortdal, V.E. In-Vitro and in-Vivo Evaluation of a Novel Bioprosthetic Pulmonary Valve for Use in Congenital Heart Surgery. *J. Cardiothorac. Surg.* **2019**, *14*, 6. [CrossRef]
7. Kuang, D.; Lei, Y.; Yang, L.; Wang, Y. Preclinical Study of a Self-Expanding Pulmonary Valve for the Treatment of Pulmonary Valve Disease. *Regen. Biomater.* **2020**, *7*, 609–618. [CrossRef]
8. Rocchi, M.; Gross, C.; Moscato, F.; Schlöglhofer, T.; Meyns, B.; Fresiello, L. An in Vitro Model to Study Suction Events by a Ventricular Assist Device: Validation with Clinical Data. *Front. Physiol.* **2023**, *14*, 1155032. [CrossRef]
9. Bozkurt, S.; van de Vosse, F.N.; Rutten, M.C.M. Enhancement of Arterial Pressure Pulsatility by Controlling Continuous-Flow Left Ventricular Assist Device Flow Rate in Mock Circulatory System. *J. Med. Biol. Eng.* **2016**, *36*, 308–315. [CrossRef]
10. Cappon, F.; Wu, T.; Papaioannou, T.; Du, X.; Hsu, P.-L.; Khir, A.W. Mock Circulatory Loops Used for Testing Cardiac Assist Devices: A Review of Computational and Experimental Models. *Int. J. Artif. Organs* **2021**, *44*, 793–806. [CrossRef]
11. Leopaldi, A.M.; Vismara, R.; Lemma, M.; Valerio, L.; Cervo, M.; Mangini, A.; Contino, M.; Redaelli, A.; Antona, C.; Fiore, G.B. In Vitro Hemodynamics and Valve Imaging in Passive Beating Hearts. *J. Biomech.* **2012**, *45*, 1133–1139. [CrossRef]
12. Granegger, M.; Aigner, P.; Kitzmüller, E.; Stoiber, M.; Moscato, F.; Michel-Behnke, I.; Schima, H. A Passive Beating Heart Setup for Interventional Cardiology Training. *Curr. Dir. Biomed. Eng.* **2016**, *2*, 735–739. [CrossRef]
13. Menne, M.F.; Grossmann, B.; Schmitz-Rode, T.; Steinseifer, U. Passive Beating Heart Platform for Testing, Training and Teaching of Transcatheter Therapies. *Struct. Heart* **2019**, *3*, 56. [CrossRef]
14. Leopaldi, A.M.; Vismara, R.; van Tuijl, S.; Redaelli, A.; van de Vosse, F.N.; Fiore, G.B.; Rutten, M.C.M. A Novel Passive Left Heart Platform for Device Testing and Research. *Med. Eng. Phys.* **2015**, *37*, 361–366. [CrossRef]
15. Park, M.H.; Zhu, Y.; Imbrie-Moore, A.M.; Wang, H.; Marin-Cuartas, M.; Paulsen, M.J.; Woo, Y.J. Heart Valve Biomechanics: The Frontiers of Modeling Modalities and the Expansive Capabilities of Ex Vivo Heart Simulation. *Front. Cardiovasc. Med.* **2021**, *8*, 673689. [CrossRef]

16. Paulsen, M.J.; Bae, J.H.; Imbrie-Moore, A.M.; Wang, H.; Hironaka, C.E.; Farry, J.M.; Lucian, H.; Thakore, A.D.; Cutkosky, M.R.; Joseph Woo, Y. Development and Ex Vivo Validation of Novel Force-Sensing Neochordae for Measuring Chordae Tendineae Tension in the Mitral Valve Apparatus Using Optical Fibers with Embedded Bragg Gratings. *J. Biomech. Eng.* **2020**, *142*, 0145011–0145019. [CrossRef]
17. de Hart, J.; de Weger, A.; van Tuijl, S.; Stijnen, J.M.A.; van den Broek, C.N.; Rutten, M.C.M.; de Mol, B.A. An Ex Vivo Platform to Simulate Cardiac Physiology: A New Dimension for Therapy Development and Assessment. *Int. J. Artif. Organs* **2011**, *34*, 495–505. [CrossRef]
18. Peper, E.S.; Leopaldi, A.M.; van Tuijl, S.; Coolen, B.F.; Strijkers, G.J.; Baan, J.; Planken, R.N.; de Weger, A.; Nederveen, A.J.; Marquering, H.A.; et al. An Isolated Beating Pig Heart Platform for a Comprehensive Evaluation of Intracardiac Blood Flow with 4D Flow MRI: A Feasibility Study. *Eur. Radiol. Exp.* **2019**, *3*, 40. [CrossRef]
19. Bozkurt, S.; van Tuijl, S.; Schampaert, S.; van de Vosse, F.N.; Rutten, M.C.M. Arterial Pulsatility Improvement in a Feedback-Controlled Continuous Flow Left Ventricular Assist Device: An Ex-Vivo Experimental Study. *Med. Eng. Phys.* **2014**, *36*, 1288–1295. [CrossRef]
20. Bozkurt, S.; van Tuijl, S.; van de Vosse, F.N.; Rutten, M.C.M. Arterial Pulsatility under Phasic Left Ventricular Assist Device Support. *Biomed. Mater. Eng.* **2016**, *27*, 451–460. [CrossRef]
21. Kondruweit, M.; Friedl, S.; Heim, C.; Wittenberg, T.; Weyand, M.; Harig, F. A New Ex Vivo Beating Heart Model to Investigate the Application of Heart Valve Performance Tools with a High-Speed Camera. *ASAIO J.* **2014**, *60*, 38. [CrossRef]
22. Pelgrim, G.J.; Das, M.; Haberland, U.; Slump, C.; Handayani, A.; van Tuijl, S.; Stijnen, M.; Klotz, E.; Oudkerk, M.; Wildberger, J.E.; et al. Development of an Ex Vivo, Beating Heart Model for CT Myocardial Perfusion. *BioMed Res. Int.* **2015**, *2015*, 412716. [CrossRef]
23. Kappler, B.; Ledezma, C.A.; van Tuijl, S.; Meijborg, V.; Boukens, B.J.; Ergin, B.; Tan, P.J.; Stijnen, M.; Ince, C.; Díaz-Zuccarini, V.; et al. Investigating the Physiology of Normothermic Ex Vivo Heart Perfusion in an Isolated Slaughterhouse Porcine Model Used for Device Testing and Training. *BMC Cardiovasc. Disord.* **2019**, *19*, 254. [CrossRef]
24. Kappler, B.; van Tuijl, S.; Ergin, B.; Fixsen, L.; Stijnen, M.; Ince, C.; de Mol, B.A. Attenuated Cardiac Function Degradation in Ex Vivo Pig Hearts. *Int. J. Artif. Organs* **2020**, *43*, 173–179. [CrossRef]
25. Schampaert, S.; van 't Veer, M.; Rutten, M.C.M.; van Tuijl, S.; de Hart, J.; van de Vosse, F.N.; Pijls, N.H.J. Autoregulation of Coronary Blood Flow in the Isolated Beating Pig Heart. *Artif. Organs* **2013**, *37*, 724–730. [CrossRef]
26. Houser, S.R.; Margulies, K.B.; Murphy, A.M.; Spinale, F.G.; Francis, G.S.; Prabhu, S.D.; Rockman, H.A.; Kass, D.A.; Molkentin, J.D.; Sussman, M.A.; et al. Animal Models of Heart Failure. *Circ. Res.* **2012**, *111*, 131–150. [CrossRef]
27. Camacho, P.; Fan, H.; Liu, Z.; He, J.-Q. Large Mammalian Animal Models of Heart Disease. *J. Cardiovasc. Dev. Dis.* **2016**, *3*, 30. [CrossRef]
28. Silva, K.A.S.; Emter, C.A. Large Animal Models of Heart Failure. *JACC Basic Transl. Sci.* **2020**, *5*, 840–856. [CrossRef]
29. Schmitto, J.D.; Ortmann, P.; Akdis, M.; Alekuzei, H.; Steinke, K.; Kolat, P.; Popov, A.F.; Liakopoulos, O.J.; Waldmann-Beushausen, R.; Mirzaie, M.; et al. Miniaturized HIA Microdiagonal Pump as Left Ventricular Assist Device in a Sheep Model. *ASAIO J.* **2008**, *54*, 233–236. [CrossRef]
30. Monreal, G.; Sherwood, L.C.; Sobieski, M.A.; Giridharan, G.A.; Slaughter, M.S.; Koenig, S.C. Large Animal Models for Left Ventricular Assist Device Research and Development. *ASAIO J.* **2014**, *60*, 2–8. [CrossRef]
31. Wang, Y.; Conger, J.L.; Handy, K.; Smith, P.A.; Cheema, F.H.; Sampaio, L.C.; Lin, F.; Chen, C.; Morgan, J.A. In Vivo Hemodynamic Evaluation of CH-VAD in a Bovine Model for 14 Days. In Proceedings of the 2018 40th Annual International Conference of the IEEE Engineering in Medicine and Biology Society (EMBC), Honolulu, HI, USA, 18–21 July 2018; Volume 2018, pp. 4512–4515. [CrossRef]
32. Kheradvar, A.; Zareian, R.; Kawauchi, S.; Goodwin, R.L.; Rugonyi, S. Animal Models for Heart Valve Research and Development. *Drug Discov. Today Dis. Models* **2017**, *24*, 55–62. [CrossRef]
33. Viceconti, M.; Henney, A.; Morley-Fletcher, E. In Silico Clinical Trials: How Computer Simulation Will Transform the Biomedical Industry. *Int. J. Clin. Trials* **2016**, *3*, 37–46. [CrossRef]
34. Hampshire, V.A.; Gilbert, S.H. Refinement, Reduction, and Replacement (3R) Strategies in Preclinical Testing of Medical Devices. *Toxicol. Pathol.* **2019**, *47*, 329–338. [CrossRef]
35. Gorzalczany, S.B.; Rodriguez Basso, A.G. Strategies to Apply 3Rs in Preclinical Testing. *Pharmacol. Res. Perspect.* **2021**, *9*, e00863. [CrossRef]
36. Shi, Y.; Lawford, P.; Hose, R. Review of Zero-D and 1-D Models of Blood Flow in the Cardiovascular System. *Biomed. Eng. OnLine* **2011**, *10*, 33. [CrossRef]
37. Shim, E.B.; Sah, J.Y.; Youn, C.H. Mathematical Modeling of Cardiovascular System Dynamics Using a Lumped Parameter Method. *Jpn. J. Physiol.* **2004**, *54*, 545–553. [CrossRef]
38. Kokalari, I.; Karaja, T.; Guerrisi, M. Review on Lumped Parameter Method for Modeling the Blood Flow in Systemic Arteries. *J. Biomed. Sci. Eng.* **2013**, *6*, 27458. [CrossRef]
39. Shimizu, S.; Une, D.; Kawada, T.; Hayama, Y.; Kamiya, A.; Shishido, T.; Sugimachi, M. Lumped Parameter Model for Hemodynamic Simulation of Congenital Heart Diseases. *J. Physiol. Sci.* **2018**, *68*, 103–111. [CrossRef]
40. Bozkurt, S. Computational Simulation of Cardiac Function and Blood Flow in the Circulatory System under Continuous Flow Left Ventricular Assist Device Support during Atrial Fibrillation. *Appl. Sci.* **2020**, *10*, 876. [CrossRef]

41. Lee, B.-K. Computational Fluid Dynamics in Cardiovascular Disease. *Korean Circ. J.* **2011**, *41*, 423–430. [CrossRef]
42. Esmailie, F.; Razavi, A.; Yeats, B.; Sivakumar, S.K.; Chen, H.; Samaee, M.; Shah, I.A.; Veneziani, A.; Yadav, P.; Thourani, V.H.; et al. Biomechanics of Transcatheter Aortic Valve Replacement Complications and Computational Predictive Modeling. *Struct. Heart* **2022**, *6*, 100032. [CrossRef] [PubMed]
43. Ghodrati, M.; Maurer, A.; Schlöglhofer, T.; Khienwad, T.; Zimpfer, D.; Beitzke, D.; Zonta, F.; Moscato, F.; Schima, H.; Aigner, P. The Influence of Left Ventricular Assist Device Inflow Cannula Position on Thrombosis Risk. *Artif. Organs* **2020**, *44*, 939–946. [CrossRef] [PubMed]
44. Taylor, C.A.; Fonte, T.A.; Min, J.K. Computational Fluid Dynamics Applied to Cardiac Computed Tomography for Noninvasive Quantification of Fractional Flow Reserve. *J. Am. Coll. Cardiol.* **2013**, *61*, 2233–2241. [CrossRef] [PubMed]
45. Morris, P.D.; Narracott, A.; von Tengg-Kobligk, H.; Silva Soto, D.A.; Hsiao, S.; Lungu, A.; Evans, P.; Bressloff, N.W.; Lawford, P.V.; Hose, D.R.; et al. Computational Fluid Dynamics Modelling in Cardiovascular Medicine. *Heart Br. Card. Soc.* **2016**, *102*, 18–28. [CrossRef] [PubMed]
46. Li, G.; Wang, H.; Zhang, M.; Tupin, S.; Qiao, A.; Liu, Y.; Ohta, M.; Anzai, H. Prediction of 3D Cardiovascular Hemodynamics before and after Coronary Artery Bypass Surgery via Deep Learning. *Commun. Biol.* **2021**, *4*, 99. [CrossRef]
47. Veronesi, F.; Corsi, C.; Caiani, E.G.; Sarti, A.; Lamberti, C. Tracking of Left Ventricular Long Axis from Real-Time Three-Dimensional Echocardiography Using Optical Flow Techniques. *IEEE Trans. Inf. Technol. Biomed.* **2006**, *10*, 174–181. [CrossRef] [PubMed]
48. El Missiri, A.M.; El Meniawy, K.A.L.; Sakr, S.A.S.; Mohamed, A.S.E. Normal Reference Values of Echocardiographic Measurements in Young Egyptian Adults. *Egypt. Heart J.* **2016**, *68*, 209–215. [CrossRef]
49. Bozkurt, S. Mathematical Modeling of Cardiac Function to Evaluate Clinical Cases in Adults and Children. *PLoS ONE* **2019**, *14*, e0224663. [CrossRef]
50. Clay, S.; Alfakih, K.; Radjenovic, A.; Jones, T.; Ridgway, J.P.; Sinvananthan, M.U. Normal Range of Human Left Ventricular Volumes and Mass Using Steady State Free Precession MRI in the Radial Long Axis Orientation. *Magn. Reson. Mater. Phys. Biol. Med.* **2006**, *19*, 41–45. [CrossRef]
51. Addetia, K.; Miyoshi, T.; Amuthan, V.; Citro, R.; Daimon, M.; Gutierrez Fajardo, P.; Kasliwal, R.R.; Kirkpatrick, J.N.; Monaghan, M.J.; Muraru, D.; et al. Normal Values of Left Ventricular Size and Function on Three-Dimensional Echocardiography: Results of the World Alliance Societies of Echocardiography Study. *J. Am. Soc. Echocardiogr. Off. Publ. Am. Soc. Echocardiogr.* **2022**, *35*, 449–459. [CrossRef]
52. Gulbulak, U.; Ertas, A. Finite Element Driven Design Domain Identification of a Beating Left Ventricular Simulator. *Bioengineering* **2019**, *6*, 83. [CrossRef] [PubMed]
53. Liu, H.; Yan, J.; Zhou, Y.; Li, H.; Li, C. A Novel Dynamic Cardiac Simulator Utilizing Pneumatic Artificial Muscle. In Proceedings of the 2013 35th Annual International Conference of the IEEE Engineering in Medicine and Biology Society (EMBC), Osaka, Japan, 3–7 July 2013; pp. 715–718.
54. Baturalp, T.B. Design and Development of a Systemic Mock Circulation Loop with a Novel Beating Left Ventricular Simulator. Ph.D. Dissertation, Texas Tech University, Lubbock, TX, USA, 2016.
55. Roche, E.T.; Wohlfarth, R.; Overvelde, J.T.B.; Vasilyev, N.V.; Pigula, F.A.; Mooney, D.J.; Bertoldi, K.; Walsh, C.J. A Bioinspired Soft Actuated Material. *Adv. Mater.* **2014**, *26*, 1200–1206. [CrossRef] [PubMed]
56. Sridar, S.; Majeika, C.J.; Schaffer, P.; Bowers, M.; Ueda, S.; Barth, A.J.; Sorrells, J.L.; Wu, J.T.; Hunt, T.R.; Popovic, M. Hydro Muscle—A Novel Soft Fluidic Actuator. In Proceedings of the 2016 IEEE International Conference on Robotics and Automation (ICRA), Stockholm, Sweden, 16–21 May 2016; pp. 4014–4021.
57. Ingels, N.B., Jr. Myocardial Fiber Architecture and Left Ventricular Function. *Technol. Health Care* **1997**, *5*, 45–52. [CrossRef] [PubMed]
58. Buckberg, G.; Mahajan, A.; Saleh, S.; Hoffman, J.I.E.; Coghlan, C. Structure and Function Relationships of the Helical Ventricular Myocardial Band. *J. Thorac. Cardiovasc. Surg.* **2008**, *136*, 578–589.e11. [CrossRef] [PubMed]
59. Buckberg, G.; Hoffman, J.I.E.; Mahajan, A.; Saleh, S.; Coghlan, C. Cardiac Mechanics Revisited: The Relationship of Cardiac Architecture to Ventricular Function. *Circulation* **2008**, *118*, 2571–2587. [CrossRef]
60. Trumble, D.R.; McGregor, W.E.; Kerckhoffs, R.C.P.; Waldman, L.K. Cardiac Assist with a Twist: Apical Torsion as a Means to Improve Failing Heart Function. *J. Biomech. Eng.* **2011**, *133*, 101003. [CrossRef]
61. Sengupta, P.P.; Tajik, A.J.; Chandrasekaran, K.; Khandheria, B.K. Twist Mechanics of the Left Ventricle: Principles and Application. *JACC Cardiovasc. Imaging* **2008**, *1*, 366–376. [CrossRef]
62. Sengupta, P.P.; Korinek, J.; Belohlavek, M.; Narula, J.; Vannan, M.A.; Jahangir, A.; Khandheria, B.K. Left Ventricular Structure and Function: Basic Science for Cardiac Imaging. *J. Am. Coll. Cardiol.* **2006**, *48*, 1988–2001. [CrossRef]
63. Sengupta, P.P.; Krishnamoorthy, V.K.; Korinek, J.; Narula, J.; Vannan, M.A.; Lester, S.J.; Tajik, J.A.; Seward, J.B.; Khandheria, B.K.; Belohlavek, M. Left Ventricular Form and Function Revisited: Applied Translational Science to Cardiovascular Ultrasound Imaging. *J. Am. Soc. Echocardiogr. Off. Publ. Am. Soc. Echocardiogr.* **2007**, *20*, 539–551. [CrossRef]
64. Ha, H.; Kim, G.B.; Kweon, J.; Lee, S.J.; Kim, Y.-H.; Kim, N.; Yang, D.H. The Influence of the Aortic Valve Angle on the Hemodynamic Features of the Thoracic Aorta. *Sci. Rep.* **2016**, *6*, 32316. [CrossRef]
65. Rotman, O.M.; Bianchi, M.; Ghosh, R.P.; Kovarovic, B.; Bluestein, D. Principles of TAVR Valve Design, Modelling, and Testing. *Expert Rev. Med. Devices* **2018**, *15*, 771–791. [CrossRef]

66. Kang, J.; Ha, H. Particle Image Velocimetry Investigation of Hemodynamics via Aortic Phantom. *J. Vis. Exp. JoVE* **2022**, *25*, e63492. [CrossRef] [PubMed]
67. Roche, E.T.; Horvath, M.A.; Wamala, I.; Alazmani, A.; Song, S.-E.; Whyte, W.; Machaidze, Z.; Payne, C.J.; Weaver, J.C.; Fishbein, G.; et al. Soft Robotic Sleeve Supports Heart Function. *Sci. Transl. Med.* **2017**, *9*, eaaf3925. [CrossRef] [PubMed]
68. Lorenzon, L.; Beccali, G.; Cianchetti, M. A Preliminary Study on an Innovative Soft Robotic Artificial Heart Ventricle. In Proceedings of the 2023 IEEE International Conference on Soft Robotics (RoboSoft), Singapore, 3–7 April 2023; pp. 1–8.
69. Shi, Y.; Korakianitis, T.; Li, Z.; Shi, Y. Structure and Motion Design of a Mock Circulatory Test Rig. *J. Med. Eng. Technol.* **2018**, *42*, 443–452. [CrossRef] [PubMed]
70. Jeong, J.-H.; Kim, Y.-M.; Lee, B.; Hong, J.; Kim, J.; Woo, S.-Y.; Yang, T.-H.; Park, Y.-H. Design and Evaluation of Enhanced Mock Circulatory Platform Simulating Cardiovascular Physiology for Medical Palpation Training. *Appl. Sci.* **2020**, *10*, 5433. [CrossRef]
71. Hendry, P.J.; Ascah, K.J.; Rajagopalan, K.; Calvin, J.E. Does Septal Position Affect Right Ventricular Function during Left Ventricular Assist in an Experimental Porcine Model? *Circulation* **1994**, *90*, II353–II358. [PubMed]
72. Flores, A.S.; Essandoh, M.; Yerington, G.C.; Bhatt, A.M.; Iyer, M.H.; Perez, W.; Davila, V.R.; Tripathi, R.S.; Turner, K.; Dimitrova, G.; et al. Echocardiographic Assessment for Ventricular Assist Device Placement. *J. Thorac. Dis.* **2015**, *7*, 2139–2150. [CrossRef] [PubMed]
73. Sack, K.L.; Dabiri, Y.; Franz, T.; Solomon, S.D.; Burkhoff, D.; Guccione, J.M. Investigating the Role of Interventricular Interdependence in Development of Right Heart Dysfunction During LVAD Support: A Patient-Specific Methods-Based Approach. *Front. Physiol.* **2018**, *9*, 520. [CrossRef] [PubMed]
74. Bravo, C.A.; Navarro, A.G.; Dhaliwal, K.K.; Khorsandi, M.; Keenan, J.E.; Mudigonda, P.; O'Brien, K.D.; Mahr, C. Right Heart Failure after Left Ventricular Assist Device: From Mechanisms to Treatments. *Front. Cardiovasc. Med.* **2022**, *9*, 1023549. [CrossRef]
75. Schampaert, S.; Pennings, K.A.M.A.; van de Molengraft, M.J.G.; Pijls, N.H.J.; van de Vosse, F.N.; Rutten, M.C.M. A Mock Circulation Model for Cardiovascular Device Evaluation. *Physiol. Meas.* **2014**, *35*, 687–702. [CrossRef]
76. De Lazzari, B.; Capoccia, M.; Badagliacca, R.; Bozkurt, S.; De Lazzari, C. IABP versus Impella Support in Cardiogenic Shock: "In Silico" Study. *J. Cardiovasc. Dev. Dis.* **2023**, *10*, 140. [CrossRef] [PubMed]
77. Alkan, R.; De Lazzari, B.; Capoccia, M.; De Lazzari, C.; Bozkurt, S. Computational Evaluation of IABP, Impella 2.5, TandemHeart and Combined IABP and Impella 2.5 Support in Cardiogenic Shock. *Mathematics* **2023**, *11*, 3606. [CrossRef]
78. Schampaert, S.; van Nunen, L.X.; Pijls, N.H.J.; Rutten, M.C.M.; van Tuijl, S.; van de Vosse, F.N.; van 't Veer, M. Intra-Aortic Balloon Pump Support in the Isolated Beating Porcine Heart in Nonischemic and Ischemic Pump Failure. *Artif. Organs* **2015**, *39*, 931–938. [CrossRef] [PubMed]
79. Granegger, M.; Mahr, S.; Horvat, J.; Aigner, P.; Roehrich, M.; Stoiber, M.; Plasenzotti, R.; Zimpfer, D.; Schima, H.; Moscato, F. Investigation of Hemodynamics in the Assisted Isolated Porcine Heart. *Int. J. Artif. Organs* **2013**, *36*, 878–886. [CrossRef] [PubMed]
80. Doke, S.K.; Dhawale, S.C. Alternatives to Animal Testing: A Review. *Saudi Pharm. J.* **2015**, *23*, 223–229. [CrossRef] [PubMed]
81. Kiani, A.K.; Pheby, D.; Henehan, G.; Brown, R.; Sieving, P.; Sykora, P.; Marks, R.; Falsini, B.; Capodicasa, N.; Miertus, S.; et al. Ethical Considerations Regarding Animal Experimentation. *J. Prev. Med. Hyg.* **2022**, *63*, E255–E266. [CrossRef] [PubMed]
82. Ferdowsian, H.R.; Beck, N. Ethical and Scientific Considerations Regarding Animal Testing and Research. *PLoS ONE* **2011**, *6*, e24059. [CrossRef] [PubMed]
83. Kiraga, Ł.; Dzikowski, A. Ethical Concerns of the Veterinarian in Relation to Experimental Animals and In Vivo Research. *Animals* **2023**, *13*, 2476. [CrossRef] [PubMed]
84. Sisakian, H. Cardiomyopathies: Evolution of Pathogenesis Concepts and Potential for New Therapies. *World J. Cardiol.* **2014**, *6*, 478–494. [CrossRef]
85. Sanz, J.; Sánchez-Quintana, D.; Bossone, E.; Bogaard, H.J.; Naeije, R. Anatomy, Function, and Dysfunction of the Right Ventricle: JACC State-of-the-Art Review. *J. Am. Coll. Cardiol.* **2019**, *73*, 1463–1482. [CrossRef]
86. Ciarambino, T.; Menna, G.; Sansone, G.; Giordano, M. Cardiomyopathies: An Overview. *Int. J. Mol. Sci.* **2021**, *22*, 7722. [CrossRef] [PubMed]
87. Díez-López, C.; Salazar-Mendiguchía, J.; García-Romero, E.; Fuentes, L.; Lupón, J.; Bayés-Genis, A.; Manito, N.; de Antonio, M.; Moliner, P.; Zamora, E.; et al. Clinical Determinants and Prognosis of Left Ventricular Reverse Remodelling in Non-Ischemic Dilated Cardiomyopathy. *J. Cardiovasc. Dev. Dis.* **2022**, *9*, 20. [CrossRef] [PubMed]
88. Tayal, U.; Prasad, S.K. Myocardial Remodelling and Recovery in Dilated Cardiomyopathy. *JRSM Cardiovasc. Dis.* **2017**, *6*, 2048004017734476. [CrossRef] [PubMed]
89. Merlo, M.; Caiffa, T.; Gobbo, M.; Adamo, L.; Sinagra, G. Reverse Remodeling in Dilated Cardiomyopathy: Insights and Future Perspectives. *Int. J. Cardiol. Heart Vasc.* **2018**, *18*, 52–57. [CrossRef] [PubMed]
90. Xie, X.; Yang, M.; Xie, S.; Wu, X.; Jiang, Y.; Liu, Z.; Zhao, H.; Chen, Y.; Zhang, Y.; Wang, J. Early Prediction of Left Ventricular Reverse Remodeling in First-Diagnosed Idiopathic Dilated Cardiomyopathy: A Comparison of Linear Model, Random Forest, and Extreme Gradient Boosting. *Front. Cardiovasc. Med.* **2021**, *8*, 684004. [CrossRef] [PubMed]
91. Sewanan, L.R.; Shimada, Y.J. Prospects for Remodeling the Hypertrophic Heart with Myosin Modulators. *Front. Cardiovasc. Med.* **2022**, *9*, 1051564. [CrossRef] [PubMed]

92. Musumeci, B.; Tini, G.; Russo, D.; Sclafani, M.; Cava, F.; Tropea, A.; Adduci, C.; Palano, F.; Francia, P.; Autore, C. Left Ventricular Remodeling in Hypertrophic Cardiomyopathy: An Overview of Current Knowledge. *J. Clin. Med.* **2021**, *10*, 1547. [CrossRef] [PubMed]
93. Zheng, Y.; Chan, W.X.; Charles, C.J.; Richards, A.M.; Sampath, S.; Abu Bakar Ali, A.; Leo, H.L.; Yap, C.H. Effects of Hypertrophic and Dilated Cardiac Geometric Remodeling on Ejection Fraction. *Front. Physiol.* **2022**, *13*, 898775. [CrossRef] [PubMed]
94. Bertini, M.; Sengupta, P.P.; Nucifora, G.; Delgado, V.; Ng, A.C.T.; Marsan, N.A.; Shanks, M.; van Bommel, R.R.J.; Schalij, M.J.; Narula, J.; et al. Role of Left Ventricular Twist Mechanics in the Assessment of Cardiac Dyssynchrony in Heart Failure. *JACC Cardiovasc. Imaging* **2009**, *2*, 1425–1435. [CrossRef]
95. Phan, T.T.; Shivu, G.N.; Abozguia, K.; Gnanadevan, M.; Ahmed, I.; Frenneaux, M. Left Ventricular Torsion and Strain Patterns in Heart Failure with Normal Ejection Fraction Are Similar to Age-Related Changes. *Eur. J. Echocardiogr.* **2009**, *10*, 793–800. [CrossRef]
96. Songsangjinda, T.; Krittayaphong, R. Impact of Different Degrees of Left Ventricular Strain on Left Atrial Mechanics in Heart Failure with Preserved Ejection Fraction. *BMC Cardiovasc. Disord.* **2022**, *22*, 160. [CrossRef] [PubMed]
97. Morimura, H.; Okamoto, Y.; Takada, J.; Tabata, M.; Iwasaki, K. Repairable Ex Vivo Model of Functional and Degenerative Mitral Regurgitation. *Eur. J. Cardio-Thorac. Surg. Off. J. Eur. Assoc. Cardio-Thorac. Surg.* **2023**, *64*, ezad371. [CrossRef] [PubMed]
98. Karl, R.; Romano, G.; Marx, J.; Eden, M.; Schlegel, P.; Stroh, L.; Fischer, S.; Hehl, M.; Kühle, R.; Mohl, L.; et al. An Ex-Vivo and in-Vitro Dynamic Simulator for Surgical and Transcatheter Mitral Valve Interventions. *Int. J. Comput. Assist. Radiol. Surg.* **2024**, *19*, 411–421. [CrossRef] [PubMed]
99. Lipshultz, S.E.; Law, Y.M.; Asante-Korang, A.; Austin, E.D.; Dipchand, A.I.; Everitt, M.D.; Hsu, D.T.; Lin, K.Y.; Price, J.F.; Wilkinson, J.D.; et al. Cardiomyopathy in Children: Classification and Diagnosis: A Scientific Statement from the American Heart Association. *Circulation* **2019**, *140*, e9–e68. [CrossRef] [PubMed]
100. Bakaya, K.; Paracha, W.; Schievano, S.; Bozkurt, S. Assessment of Cardiac Dimensions in Children Diagnosed with Hypertrophic Cardiomyopathy. *Echocardiography* **2022**, *39*, 1233–1239. [CrossRef] [PubMed]
101. Lesage, R.; Van Oudheusden, M.; Schievano, S.; Van Hoyweghen, I.; Geris, L.; Capelli, C. Mapping the Use of Computational Modelling and Simulation in Clinics: A Survey. *Front. Med. Technol.* **2023**, *5*, 1125524. [CrossRef]
102. Yoo, S.-J.; Spray, T.; Austin, E.H.; Yun, T.-J.; van Arsdell, G.S. Hands-on Surgical Training of Congenital Heart Surgery Using 3-Dimensional Print Models. *J. Thorac. Cardiovasc. Surg.* **2017**, *153*, 1530–1540. [CrossRef]